

Position Control of a 3 dof Closed-loop Cylinder System Using ER Valve Actuators

Seung-Bok Choi and Myung-Soo Cho

Department of Mechanical Engineering, Inha University, Incheon, South Korea

ABSTRACT

This paper presents the position tracking control of a closed-loop cylinder system using electro-rheological(ER) valve actuators. After manufacturing three sets of cylindrical ER valves on the basis of Bingham model of ER fluid, a 3 dof(degree-of-freedom) closed-loop cylinder system having the heave, roll and pitch motions is constructed. The governing equations of motion are derived using Lagrange's equation and a control model is formulated by considering nonlinear characteristics of the system. Sliding mode controllers are then designed for these ER valve actuators in order to achieve position tracking control. The effectiveness of trajectory tracking control performance of the proposed cylinder system is demonstrated through computer simulation and experimental implementation of the sliding mode controller.

Keywords : Electro-Rheological Fluid, ER Valve, Closed-loop Cylinder System, Position Control, Sliding Mode Control

1. Introduction

Recently, a great attention has been given to parallel link manipulators and their applications⁽¹⁻⁴⁾. The parallel link manipulator consisting of the moving platform and the base platform has several advantages compared with a serial link manipulator such as higher structure rigidity and heavier load tasks. Most of parallel link manipulators are activated by hydraulic servo valves. In order to increase both accuracy and time response various types of valves have been widely devised as key elements in hydraulic control system^(5,6). However, the servo valve is complex and expensive. Hence, it is desirable to introduce an alternative means of actuating mechanisms. One of new approaches to achieve this goal is to use an electro-rheological (ER) fluid. On the basis of the fact that rheological properties of the ER fluid are reversibly and instantaneously changed by applying the electric field to the fluid domain, numerous research activities have been performed in various engineering applications. These includes shock absorbers, engine mounts,

clutch/brake systems, intelligent structures and valves.

When the ER fluid is employed in valve systems, the pressure drop of control volume can be continuously tuned by controlling the intensity of the electric field. This inherent feature of the ER fluid has triggered considerable research activities in the development of valve devices. Simmonds⁽⁷⁾ proposed a plate-type ER valve and investigated the pressure drop responses of the ER valve with respect to the electric field. Brooks⁽⁸⁾ carried out an experiment on the pressure drop through ER valve circuits and described potential applications of the valve systems to various engineering devices. Nakano and Yonekawa⁽⁹⁾ analyzed the flow of an ER fluid passing through a plate-type ER valve as the Hagen-Poiseuille flow, and also observed compressible effect on the pressure drop of the ER valve under imposed electric potentials. Whittle et al.⁽¹⁰⁾ formulated a dynamic model of second-order system for the analysis of the pressure drop of an ER valve, and experimentally proved the validity of the model. More recently, Choi et al.⁽¹¹⁾ proposed a neural network control scheme and experimentally implemented it for the position control of

a single-rod cylinder system using ER valves. Other recent studies are well described in the survey literature⁽¹²⁾. As evident from these previous works, so far most of researches for the ER valve have focused only on the modeling and performance analysis of the field-dependent pressure drop. Researches on the position control of a multi-degree-of-freedom system or mechanism using ER valves are considerably rare. Consequently, the main contribution of this paper is to show how ER valve actuators can be satisfactorily employed for the position control of a 3 degree-of-freedom (d.o.f.) closed-loop cylinder system subjected to variable load on the moving end-effector. The effectiveness of the proposed control system is confirmed by both simulation and experimental results.

To demonstrate this, cylindrical ER valves are designed and manufactured on the basis of experimentally obtained Bingham model of a chemically treated starch/silicone oil-based ER fluid. A 3 d.o.f. closed-loop cylinder system activated by three sets of ER valve bridge circuits is then constructed, and its kinematic and dynamic equations are derived. Sliding mode controllers for heave, roll and pitch motions are formulated by treating variable load on the moving end-effector as parameter uncertainty. The controllers are then experimentally realized to provide position tracking responses in time domain.

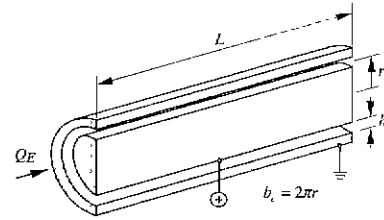
2. System Modeling

2.1 ER valve actuator

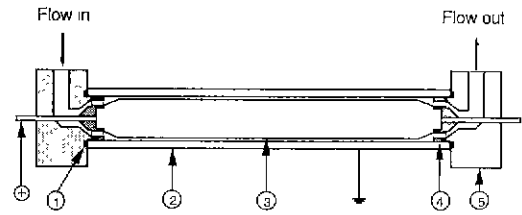
Rheological properties of ER fluid can be reversibly changed depending upon the imposition of the electric field. The ER fluid is changed from near Newtonian flow in which particles move freely to Bingham behavior in which particles are aligned in a chain by applying the electric field. Under the electric potential, a constitutive equation for the ER fluid has approximately form of Bingham plastic⁽¹³⁾:

$$\tau_f = \tau_y(E) + \eta\dot{\gamma} \quad \text{with} \quad \tau_y(E) = \alpha E^\beta \quad (1)$$

Here τ_f is shear stress, η is viscosity, $\dot{\gamma}$ is shear rate, and $\tau_y(E)$ is yield stress of the ER fluid. As evident from Eq. (1), $\tau_y(E)$ is a function of the electric field of E and



(a) geometry



① 'O' Ring ② Outer Electrode ③ Inner Electrode ④ Fixture ⑤ Cover

(b) assembly

Fig. 1 The proposed ER valve

exponentially increases with respect to the electric field. The proportional coefficient, α , and the exponent, β are intrinsic values of the ER fluid to be experimentally determined.

In this study, for the ER fluid, chemically-treated starch and silicone oil are chosen as particle and liquid, respectively. The viscosity of the base oil is 30cSt. The size of the particles ranges from 26 μm to 88 μm . The weight ratio of the particles to the ER fluid is 30 %. A commercial electroviscometer (Haake, VT-500) is employed to obtain Bingham property of the ER fluid. The testing temperature of the ER fluid is set to 55°C by considering operation conditions of the proposed control system. The yield stress $\tau_y(E)$ is obtained by $1.44.6E^{1.77}$ Pa as the form of Eq. (1). Here, the unit of E is kV/mm .

A geometry of a cylindrical ER valve devised in this work is shown in Fig. 1(a). The pressure drop ΔP_T of the ER valve in the presence of the electric field is obtained by adding the pressure drop due to the viscosity ΔP_η and the pressure drop due to the ER effect ΔP_{Lx} associated with the yield stress. In case the electrode gap h is much smaller than the radius r , the pressure drop of the cylindrical ER valve can be approximately obtained by the following equations^(11,14).

$$\Delta P_L = \Delta P_{ER} + \Delta P_\eta \quad (2)$$

where,

$$\Delta P_{ER} = 2 \frac{L}{h} \tau_v(E), \quad \Delta P_{\eta} = 12\eta \frac{L}{b_e h^3} Q_E \quad (3)$$

In the above, L is the electrode length. $b_e (= 2\pi r)$ is the effective width of the electrode, and Q_E is the flow passing through the electrode gap under the imposed electric field. By incorporating experimentally obtained Bingham model with Eq. (3), the pressure drop can be evaluated with respect to the intensity of the electric field and design parameters. Fig. 1(b) shows the assembly drawing of the manufactured ER valve. The material for the outer electrode(②) is stainless steel, while 45C steel for the inner electrode(③). The fixture(④) is used to maintain the electrode gap, and the ‘O’ ring(①) is adopted to prevent the leakage of the ER fluid. Geometrical dimensions of the gap(h), radius(r) and length(L) are 0.8 mm, 12.1 mm and 200 mm, respectively.

A hydraulic bridge circuit with four ER valves is shown in Fig. 2. The ER valves 1 and 3 are electrically connected, while the ER valves 2 and 4 are connected. The control electric field to be applied to the valves 1 and 3 is denoted by E_1 , while E_2 for the valves 2 and 4. The $Q_i (i=1,2,3,4)$ represents a flow rate of the corresponding valve. Now, using equivalent hydraulic laws to Kirchoffs’ law for an electric circuit, the following equations for pressure drops are obtained.⁽⁷⁾

$$\begin{aligned} P_1 - P_a &= RQ_1 + \Delta P_{ER}(E_1) \\ P_1 - P_b &= RQ_2 + \Delta P_{ER}(E_2) \\ P_a - P_2 &= RQ_4 + \Delta P_{ER}(E_2) \\ P_b - P_2 &= RQ_3 + \Delta P_{ER}(E_1) \\ Q &= Q_1 + Q_2 = Q_3 + Q_4 \end{aligned} \quad (4)$$

In the above, $R = 12\eta L / b_e h^3$. Assuming that four ER valves are exactly same, we can derive the following equations from Eq. (4).

$$\begin{aligned} P_a &= \frac{1}{2} (P_1 + P_2 - R(Q_1 - Q_4) - \Delta P_{ER}(E_1) + \Delta P_{ER}(E_2)) \\ P_b &= \frac{1}{2} (P_1 + P_2 + R(Q_3 - Q_2) + \Delta P_{ER}(E_1) - \Delta P_{ER}(E_2)) \end{aligned} \quad (5)$$

From the above equations, we easily know that the pressures P_a and P_b can be controlled by the terms of $\Delta P_{ER}(E_i)$ as a function of the electric field E_i .

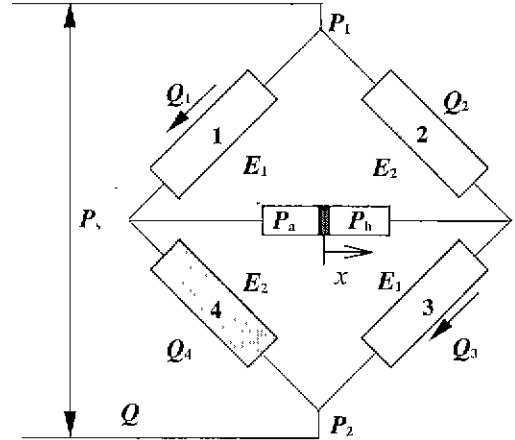


Fig. 2 ER valve bridge circuit

On the other hand, from the generalized flow continuity equations⁽¹⁵⁾ we can derive the following dynamic equations.

$$\begin{aligned} Q_1 - Q_4 &= A\dot{x} + C_a \frac{dP_a}{dt}, \quad C_a = \frac{V_a}{\beta_{ER}} \\ Q_3 - Q_2 &= A\dot{x} + C_b \frac{dP_b}{dt}, \quad C_b = \frac{V_b}{\beta_{ER}} \\ C_a &\cong C_b \cong C = \frac{V_a + V_b}{2\beta_{ER}} \end{aligned} \quad (6)$$

Here, V_a and V_b are volumes of the control volumes a and b , respectively. The term β_{ER} is the bulk modulus of the ER fluid. Now, substituting Eq. (6) into Eq. (5), and defining the pressure drop $\Delta P = P_a - P_b$, yield the following dynamic equation.

$$\frac{d(\Delta P)}{dt} = -\frac{2}{RC} \Delta P - \frac{2A}{C} \dot{x} - \frac{2}{RC} [\Delta P_{ER}(E_1) - \Delta P_{ER}(E_2)] \quad (7)$$

It is noted that the pressure drop $\Delta P_{ER}(E_1)$, $\Delta P_{ER}(E_2)$ are always positive, since the pressure drop only increases as the electric field increases. Moreover, we know that only one kind of ER fluid is used for actuating. Therefore, we can consider the system given by Eq. (7) as a single input system by taking into account the direction of the motion as follows.

$$\begin{aligned} \text{When } \dot{x} > 0, \quad \Delta P_{ER}(E_2) > 0 \text{ and } \Delta P_{ER}(E_1) = 0 \\ \text{When } \dot{x} < 0, \quad \Delta P_{ER}(E_1) > 0 \text{ and } \Delta P_{ER}(E_2) = 0 \end{aligned} \quad (8)$$

Three set of ER valve actuators featuring the bridge circuits of Eqs. (7) and (8) are manufactured for the motion control of a 3 d.o.f. closed-loop cylinder system.

2.2 3 d.o.f. cylinder system

A 3 d.o.f. closed-loop cylinder system proposed in this work is shown in Fig. 3. The system consists of two platforms; a moving platform and a base platform. And three identical legs, each including spherical or/and pin joints, connect the platforms. Thus, we have 3 d.o.f. motion for heave (T), roll (θ_r) and pitch (θ_p) by actuating the hydraulic cylinder legs. For the kinematic analysis of the proposed system, we first obtain the following equations which represent the relationship between input displacement (l_1, l_2, l_3) and output position/orientation (T, θ_r, θ_p).

$$\begin{aligned} l_1^2 &= (b - p \cos \theta_r)^2 + (T + p \sin \theta_r)^2 \\ l_2^2 &= (b - p \cos \theta_r)^2 + (T - p \sin \theta_r)^2 \\ l_3^2 &= (b - p \cos \theta_p)^2 + (p \sin \theta_p \sin \theta_r)^2 \\ &\quad + (T + p \sin \theta_p \cos \theta_r)^2 \end{aligned} \quad (9)$$

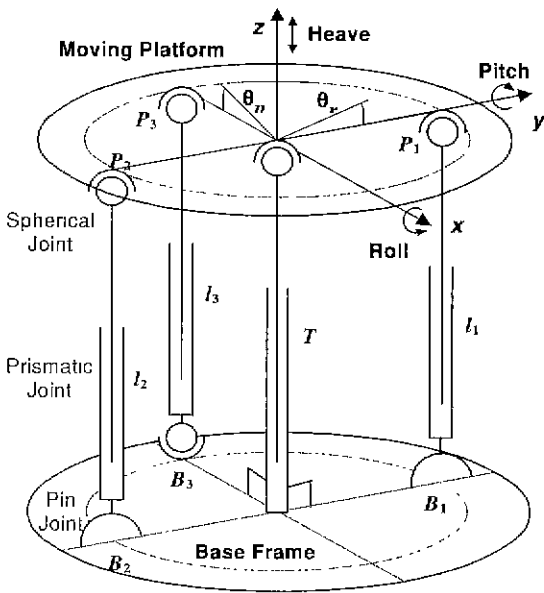


Fig. 3 The proposed 3 d.o.f. closed-loop cylinder system

In the above, b is the distance from base center to joint B_i , and p is the distance from the center of the

moving platform to joint p_i . Now, by differentiating Eq. (9), we obtain the following velocity equations between the input and output.

$$\begin{bmatrix} \dot{l}_1 \\ \dot{l}_2 \\ \dot{l}_3 \end{bmatrix} = J \begin{bmatrix} \dot{T} \\ \dot{\theta}_r \\ \dot{\theta}_p \end{bmatrix} \equiv J \begin{bmatrix} \dot{x}_1 \\ \dot{x}_2 \\ \dot{x}_3 \end{bmatrix}, \quad J = \begin{bmatrix} j_{11} & j_{12} & j_{13} \\ j_{21} & j_{22} & j_{23} \\ j_{31} & j_{32} & j_{33} \end{bmatrix} \quad (10)$$

where,

$$\begin{aligned} j_{11} &= (T + p \sin \theta_r) / l_1 \\ j_{12} &= (pb \sin \theta_r + T p \cos \theta_r) / l_1 \\ j_{13} &= 0 \\ j_{21} &= (T - p \sin \theta_r) / l_2 \\ j_{22} &= (pb \sin \theta_r - T p \cos \theta_r) / l_2 \\ j_{23} &= 0 \\ j_{31} &= (T + p \cos \theta_r \sin \theta_p) / l_3 \\ j_{32} &= (-T p \sin \theta_r \sin \theta_p) / l_3 \\ j_{33} &= (pb \sin \theta_p + T p \cos \theta_r \cos \theta_p) / l_3 \end{aligned} \quad (11)$$

In the above, J is Jacobian matrix. It is noted that output variables in Eq. (10) are defined by $[x_1 \ x_2 \ x_3]^T = [T \ \theta_r \ \theta_p]^T$. On the other hand, we can also derive force/moment equations from the virtual work principle by using the Jacobian matrix J as follow⁽⁴⁾.

$$\begin{bmatrix} F_{cz} \\ M_{cx} \\ M_{cy} \end{bmatrix} = J^T \begin{bmatrix} A \cdot \Delta P_1 \\ A \cdot \Delta P_2 \\ A \cdot \Delta P_3 \end{bmatrix} \equiv J^T \begin{bmatrix} u_1 \\ u_2 \\ u_3 \end{bmatrix} \quad (12)$$

Here, F_{cz} is the control force in the z direction, and M_{cx} and M_{cy} represent control moments in the x and y directions, respectively. The term ΔP_i in Eq. (12) is the pressure drop of the ER valve actuator given by Eq. (7). It is seen from Eq. (12) that the design of appropriate controller u_i directly implies the control of the pressure drop, which is accomplished by applying appropriate control electric fields to the ER valve actuator.

Now, to derive the dynamic equations of motion for the proposed closed-loop cylinder system, we first obtain the following kinetic (K) and potential (P) energies.

$$K = \frac{1}{2} (m\dot{T}^2 + I_r \cos^2 \theta_p \dot{\theta}_r^2 + I_y \dot{\theta}_p^2), \quad P = mgT \quad (13)$$

where m is the mass of the moving platform. g is the gravitational acceleration, and I_x and I_y represent the moment of inertia of the moving platform about x and y axis, respectively. Substituting Eq. (13) into Lagrange equation yields the following governing equations of motion.

$$\begin{aligned} \frac{d}{dt}[m\dot{T}] + mg &= F_{cz} = j_{11}u_1 + j_{21}u_2 + j_{31}u_3 \\ \frac{d}{dt}[I_x \cos^2\theta_p \dot{\theta}_r] &= M_{cx} = j_{12}u_1 + j_{22}u_2 + j_{32}u_3 \\ \frac{d}{dt}[I_y \dot{\theta}_p] + (I_x \cos\theta_p \sin\theta_p) \dot{\theta}_r^2 &= M_{cy} = j_{33}u_3 \end{aligned} \quad (14)$$

In practice, the mass of the moving platform is subjected to be varied due to the change of load conditions, and hence we rewrite Eq. (14) by considering parameter uncertainty as follows.

$$\begin{aligned} \frac{d}{dt}[m_e \dot{T}] + m_e g &= F_{cz} = j_{11}u_1 + j_{21}u_2 + j_{31}u_3 \\ \frac{d}{dt}[I_{xe} \cos^2\theta_p \dot{\theta}_r] &= M_{cx} = j_{12}u_1 + j_{22}u_2 + j_{32}u_3 \\ \frac{d}{dt}[I_{ye} \dot{\theta}_p] + (I_{xe} \cos\theta_p \sin\theta_p) \dot{\theta}_r^2 &= M_{cy} = j_{33}u_3 \end{aligned} \quad (15)$$

where,

$$m_e = m_o + \Delta m, \quad I_{xe} = I_{xo} + \Delta I_x, \quad I_{ye} = I_{yo} + \Delta I_y \quad (16)$$

In the above, m_o, I_{xo} and I_{yo} are nominal values, while $\Delta m, \Delta I_x$ and ΔI_y are corresponding uncertain parts.

By assuming so-called matching condition⁽¹⁶⁾, these uncertainties can be expressed by

$$\begin{aligned} \frac{1}{m_o + \Delta m} &= \frac{1}{m_o} (1 + \gamma_1), \quad |\gamma_1| < \phi_1 < 1 \\ \frac{1}{I_{xo} + \Delta I_x} &= \frac{1}{I_{xo}} (1 + \gamma_2), \quad |\gamma_2| < \phi_2 < 1 \\ \frac{1}{I_{yo} + \Delta I_y} &= \frac{1}{I_{yo}} (1 + \gamma_2), \quad |\gamma_2| < \phi_2 < 1 \end{aligned} \quad (17)$$

The matching condition physically implies that the input uncertain part $\Delta m, \Delta I_x, \Delta I_y$ can not have arbitrarily large perturbation.

3. Sliding Mode Controller

It is generally difficult to model the hydraulic system and design a robust controller precisely, because the hydraulic system contains internal and external uncertainties, and nonlinearity. So, a sliding mode controller, which has inherent robustness to system uncertainties, nonlinearity and internal/external disturbances, is adopted to achieve robust tracking control performance. In order to formulate a sliding mode controller, we first define tracking error as follow^(17,18).

$$e_i = x_i - x_{i-d}, \quad \dot{e}_i = \dot{x}_i - \dot{x}_{i-d} \quad i=1,2,3 \quad (18)$$

where x_{i-d} and \dot{x}_{i-d} are desired position and velocity, respectively. The problem now is to design sliding surfaces that guarantee stable sliding mode motions. Using the pole-placement method, we construct the stable sliding surfaces for the proposed system as follows.

$$s_k = \sum_{i=1}^3 (C_{k(i)} \cdot e_i + C_{k(i+3)} \cdot \dot{e}_i) \quad k=1,2,3 \quad (19)$$

Then, in order to guarantee that the tracking variables e_i and \dot{e}_i of the system are constrained to the sliding surfaces during the sliding motions, the following sliding mode condition is introduced

$$s_k \cdot \dot{s}_k < 0 \quad (20)$$

Now, we propose a sliding mode controller given by

$$\begin{aligned} u_k &= -\sum_{i=1}^3 \frac{1}{1-\phi_i} \{ C_{k(i)} (|\dot{x}_i| + |\dot{x}_{i-d}|) + C_{k(i+3)} |\ddot{x}_{i-d}| + \\ &C_{k(5)} |2\tan x_3 \dot{x}_2 \cdot \dot{x}_3| + C_{k(6)} |\cos x_3 \sin x_3 \dot{x}_2^2| \} \text{sgn}(s_k) \\ &- K_k \text{sgn}(s_k) \end{aligned} \quad (21)$$

where K_k is a discontinuous gain. Then, we can show that the uncertain system with the proposed controller satisfies the sliding mode condition as follows⁽¹⁸⁾.

$$\begin{aligned}
 s_k \cdot s_k = & \sum_{i=1}^3 \left\{ \left(C_{k(i)} (\dot{x}_i - \dot{x}_{i,d}) s_k - \frac{1+\gamma_i}{1-\phi_i} C_{k(i)} (|x_i| + |\dot{x}_{i,d}|) |s_k| \right) \right. \\
 & \left. + \left(-C_{k(i)} \dot{x}_{i,d} s_k - \frac{1+\gamma_i}{1-\phi_i} C_{k(i)} |\dot{x}_{i,d}| |s_k| \right) \right\} \\
 & \left(C_{k(5)} 2 \tan x_3 \dot{x}_2 \cdot \dot{x}_3 \cdot s_k - \frac{1+\gamma_2}{1-\phi_2} C_{k(5)} |2 \tan x_3 \dot{x}_2 \cdot \dot{x}_3| |s_k| \right) + \\
 & \left(-C_{k(6)} \cos x_3 \sin x_3 \dot{x}_2^2 s_k - \frac{1+\gamma_3}{1-\phi_3} C_{k(6)} |\cos x_3 \sin x_3 \dot{x}_2^2| |s_k| \right) < 0
 \end{aligned} \tag{22}$$

To alleviate the chattering in the control action, we replace the sign function in Eq. (21) by nonlinear saturation function as follows.

$$\text{sat}(s_k / \varepsilon_k) = \begin{cases} s_k / \varepsilon_k \cdot |s_k / \varepsilon_k| \leq 1 \\ \text{sgn}(s_k) \cdot |s_k / \varepsilon_k| > 1 \end{cases} \tag{23}$$

where ε_k is the boundary layer thickness. Once the control input is achieved from Eq.(21), control electric fields to be applied to the ER valve actuators are determined as follows.

$$\begin{aligned}
 u_k = & \Delta P_{ER}(E_2) - \Delta P_{ER}(E_1) = 2 \frac{L}{h} [\tau_x(E_2) - \tau_x(E_1)] \\
 = & \text{sgn}(u_k) \times 2 \frac{L}{h} \times 144.6 |E_2 - E_1|^{1.77}
 \end{aligned} \tag{24}$$

4. Results and Discussions

An experimental configuration for the accomplishment of the position tracking control of the proposed manipulator is presented in Fig. 4. The instrumentation largely consists of two parts: moving and control parts. The geared pump is used to make the ER fluid flow. The control part consists of sensors, microcomputer, signal conditioners and high voltage amplifier. Three LVDT sensors are used to measure the length of legs, and the position/orientation of end-effector are calculated from kinematic equations. The calculated control variables are computed with desired ones, and control electric fields to minimize the tracking errors are applied to the ER valve actuators via three sets of high voltage amplifiers. Consequently, an accurate position tracking control of the closed-loop cylinder system is achieved. In the controller implementation, the operating temperature of the ER fluid is controlled to be maintained at 55°C, and the flow rate of the ER fluid from the pump is set by 55 l/min. The sampling rate is chosen by 1000 samples/sec for A/D and D/A converters. The system and control parameters employed for both computer simulation and experimental realization are as follows : $m_0 = 3.0 \text{ kg}$, $I_{y0} = I_{z0} = 1.04e-3 \text{ kg m}^2$, $K_1 = K_2 = 80$, $K_3 = 300$, $\phi_i = 0.7$, $\varepsilon_1 = \varepsilon_2 = 0.7$, $\varepsilon_3 = 0.5$.

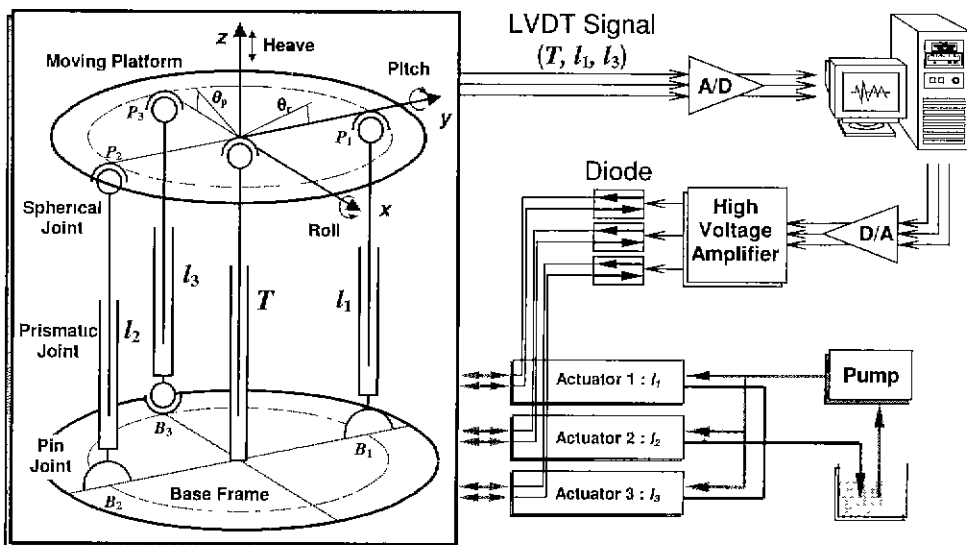


Fig. 4 Experimental configuration for position control

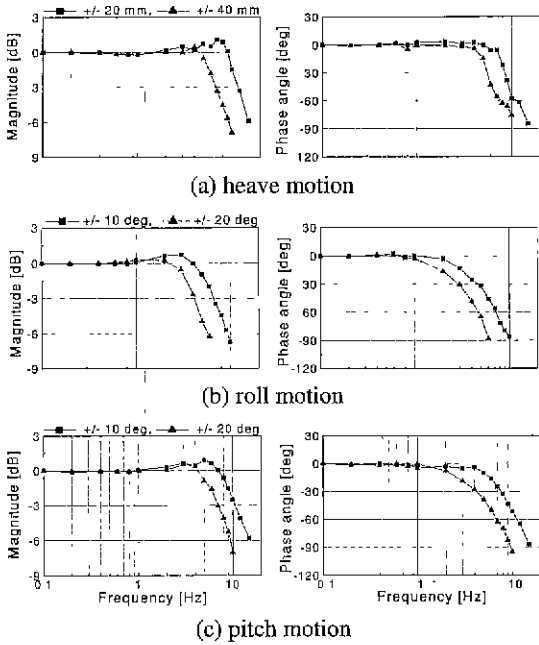


Fig. 5 Bode plots of each motion of the cylinder system

Fig. 5 shows the bode plots of a 3 d.o.f. closed-loop cylinder system. It is seen that the heave motion has a wider bandwidth than any other motions, because the proposed parallel structure has a large force transmissionability to z-direction. Fig. 6, Fig. 7 present simulated and measured position tracking control response for the desired heave motion only given by

$$\begin{aligned} T_d &= 15\sin(2\pi t) \quad [\text{mm}] \\ \theta_{r,d} &= \theta_{p,d} = 0 \quad [\text{deg}] \end{aligned} \quad (25)$$

It is observed that the tracking error is very small in the heave motion by applying control field determined from the proposed sliding mode controller. It is noted that we have nonzero tracking error in the pitching motion. This is risen from that the heave motion is asymmetrically activated with respect to the pitch axis. We also see that the simulation results agree well to the measured ones, thus proving the validity of the proposed dynamic model as well as control scheme.

Fig. 8 shows measured position tracking control response for the 2 Hz pitch motion only. it is observed that the tracking control performances are favorable with the SMC. For more complicated motions of the platform, the following desired trajectories for the heave, roll and pitch motions are chosen :

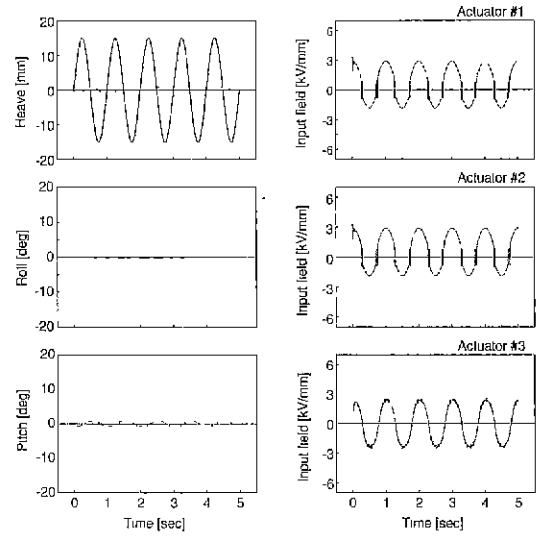


Fig. 6 Position tracking responses for heave motion only; simulated (— desired actual - - - - error)

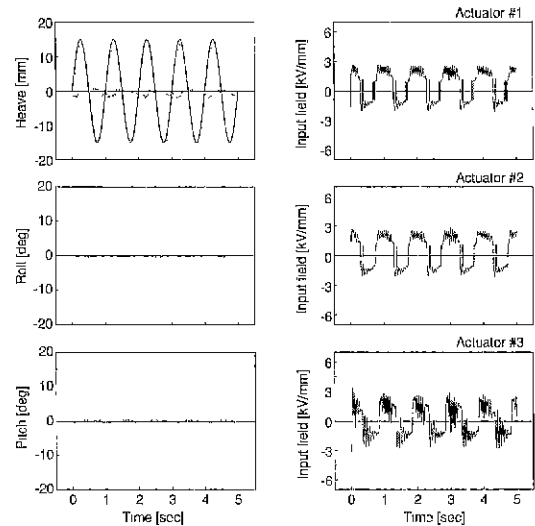


Fig. 7 Position tracking responses for heave motion only; measured (— desired actual - - - - error)

$$\begin{aligned} T_d &= 15\sin(2\pi t) \quad [\text{mm}] \\ \theta_{r,d} &= 5\sin(2\pi t) \quad [\text{deg}] \\ \theta_{p,d} &= 15\sin(2\pi t + \pi) \quad [\text{deg}] \end{aligned} \quad (26)$$

Fig. 9 presents measured tracking control response obtained using the proposed sliding mode controller (SMC). We clearly observe that the imposed desired trajectories of the motions are favorably tracked by real ones without significant tracking errors. It is noted that

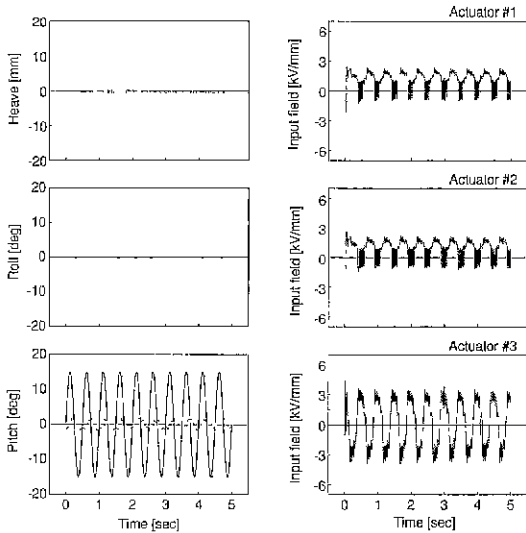


Fig. 8 Position tracking responses for pitch motion only; measured (— desired actual - - - - - error)

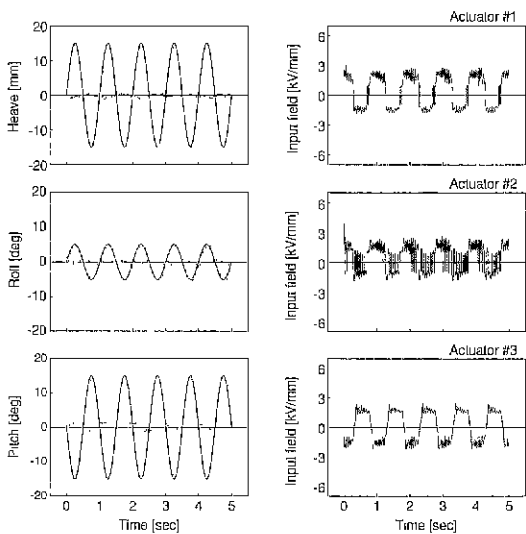


Fig. 9 Position tracking responses for heave, roll and pitch motions; measured (— desired actual - - - - - error)

the negative control electric field implies the opposite direction of the velocity component of each motion.

5. Conclusions

The position tracking control responses of a 3 d.o.f. closed-loop cylinder system activated by electro-rheological valves have been presented in this work.

Cylindrical ER valves were firstly designed and manufactured on the basis of the field-dependent Bingham model. The ER valve actuator model was then formulated and its dynamic equation was derived. For the proposed 3 d.o.f. closed-loop cylinder system which has the heave, roll and pitch motions, the kinematic relations were analyzed and the governing equations of motions were derived using Lagrange's equation. The control model was then established by considering variable load on the end-effector as uncertain parameter. A sliding mode controller which has inherent robustness to system uncertainties was designed to achieve robust tracking control performance, and favorable tracking control results for various trajectories were obtained through both computer simulation and experimental implementation. The results presented in this study are quite self-explanatory justifying that the ER valve bridge-cylinder system incorporating the sliding mode controller is very useful for many relevant engineering applications including hydraulic servo-systems such as robot manipulators and active suspension systems.

References

1. E. F. Fichter, "A Stewart Platform-Based Manipulator : General Theory and Practical Construction," *The International Journal of Robotics Research*, Vol. 5, No. 2, pp. 157-182, 1986.
2. K. M. Lee and D. K. Shah, "Dynamic Analysis of a Three-Degree-of-Freedom In-Parallel Actuated Manipulator," *IEEE Transactions on Robotics and Automation*, Vol. 4, No. 3, pp. 361-367, 1988.
3. G. Leuret, K. Liu and F. L. Lewis, "Dynamic Analysis and Control of a Stewart Platform Manipulator," *Journal of Robotic Systems*, Vol. 10, No. 5, pp. 629-655, 1993.
4. K. Kosuge, M. Okuda, H. Kawamata and T. Fukuda, "Input/Output Force Analysis of Parallel Link Manipulators," *Proceedings of the IEEE Int. Conf. on Robotics and Automation*, Vol. 1, pp. 714-719, 1993.
5. J. Watton, "The Dynamic Performance of an Electrohydraulic Servo Valve/Motor System with Transmission Line Effects," *ASME Journal of Dynamic Systems, Measurement, and Control*, Vol. 109, pp. 14-18, 1987.

6. A. R. Plummer and N. D. Vaughan, "Robust Adaptive Control for Hydraulic Servosystems." *ASME Journal of Dynamic Systems, Measurement, and Control*, Vol. 118, pp. 237-244, 1996.
7. A. J. Simmonds, "Electro-Rheological Valves in a Hydraulic Circuit," *IEE Proceeding-D*, Vol. 138, No. 4, pp. 400-404, 1991.
8. D. A. Brooks, "Design and Development of Flow Based Electro-Rheological Devices," *Journal of Modern Physics*, Vol. 6, pp. 2705-2730, 1992.
9. M. Nakano and T. Yonekawa, "Pressure Response of ER Fluid in a Piston Cylinder-ER Valve System," *Proceedings of the Fourth International Conference on Electrorheological Fluids*, pp. 477-489, 1994.
10. M. Whittle, R. Firoozian and W. A. Bullough, "Decomposition of the Pressure in an ER Valve Control System," *Journal of Intelligent Material Systems and Structures*, Vol. 5, No. 1, pp. 105-111, 1994.
11. S. B. Choi, C. C. Cheong, J. M. Jung and Y. T. Choi, "Position Control of an ER Valve-Cylinder System via Neural Network Controller," *Mechatronics*, Vol. 7, No. 1, pp. 37-52, 1997.
12. N. D. Sims, R. Stanway and A. R. Johnson, "Vibration Control Using Smart Fluids : a state-of-the-art review." *The Shock and Vibration Digest*, Vol. 31, No. 3, pp. 195~203, 1999.
13. P. M. Adriani and A. P. Gast, "A Microscopic Model of Electrorheology," *Physics of Fluids*, Vol. 31, No. 10, pp. 2757-2768, 1988.
14. R. W. Phillips, "Engineering Applications of Fluids with a Variable Yield Stress." *Ph. D. Thesis, Dept. of Mechanical Engineering*, University of California at Berkeley, 1969.
15. J. Watton, "*Fluid Power System*," Prentice Hall, Englewood Cliffs, NJ, 1989.
16. G. Leitmann, "On the Efficacy of Nonlinear Control in Uncertain Linear Systems," *ASME Journal of Dynamic Systems, Measurement, and Control*, Vol. 102, pp. 95-102, 1981.
17. J. J. E. Slotine and W. Li, "*Applied Nonlinear Control*," Prentice Hall, Englewood Cliffs, NJ, 1991.
18. D. W. Park and S. B. Choi, "Moving Sliding Surface for High-Order Variable Structure Systems," *International Journal of Control*, Vol. 72, No. 11, pp. 960-970, 1999.